eNeuro

Research Article: New Research

Cognition and Behavior

Visual Working Memory Recruits Two Functionally Distinct Alpha Rhythms in Posterior Cortex

Julio Rodriguez-Larios,[1,2] Alma ElShafei,[3] Melanie Wiehe,[3] and Saskia Haegens[1,2,3]

https://doi.org/10.1523/ENEURO.0159-22.2022

[1]Department of Psychiatry, Columbia University, New York, NY, 10032, [2]Division of Systems Neuroscience, New York State Psychiatric Institute, New York, NY, 10032, and [3]Donders Institute for Brain, Cognition and Behavior, Radboud University, Nijmegen, 6525 EN, The Netherlands

Abstract

Oscillatory activity in the human brain is dominated by posterior alpha oscillations (8–14 Hz), which have been shown to be functionally relevant in a wide variety of cognitive tasks. Although posterior alpha oscillations are commonly considered a single oscillator anchored at an individual alpha frequency (~10 Hz), previous work suggests that individual alpha frequency reflects a spatial mixture of different brain rhythms. In this study, we assess whether independent component analysis (ICA) can disentangle functionally distinct posterior alpha rhythms in the context of visual short-term memory retention. Magnetoencephalography (MEG) was recorded in 33 subjects while performing a visual working memory task. Group analysis at sensor level suggested the existence of a single posterior alpha oscillator that increases in power and decreases in frequency during memory retention. Conversely, single-subject analysis of independent components revealed the existence of two dissociable alpha rhythms: one that increases in power during memory retention (Alpha1) and another one that decreases in power (Alpha2). Alpha1 and Alpha2 rhythms were differentially modulated by the presence of visual distractors (Alpha1 increased in power while Alpha2 decreased) and had an opposite relationship with accuracy (positive for Alpha1 and negative for Alpha2). In addition, Alpha1 rhythms showed a lower peak frequency, a narrower peak width, a greater relative peak amplitude and a more central source than Alpha2 rhythms. Together, our results demonstrate that modulations in posterior alpha oscillations during short-term memory retention reflect the dynamics of at least two distinct brain rhythms with different functions and spatiospectral characteristics.

Key words: alpha oscillations; attention; MEG; memory

Significance Statement

alpha Oscillations are the most prominent feature of the human brain's electrical activity, and consist of rhythmic neuronal activity in posterior parts of the cortex. alpha Is usually considered a single brain rhythm that changes in power and frequency to support cognitive operations. We here show that posterior alpha entails at least two dissociable rhythms with distinct functions and characteristics. These findings could solve previous inconsistencies in the literature regarding the direction of task-related alpha power/frequency modulations and their relation to cognitive performance. In addition, the existence of two distinct posterior alpha rhythms could have important consequences for the design of neurostimulation protocols aimed at modulating alpha oscillations and subsequently cognition.

Introduction

Working memory entails the storage of information over brief periods of time for its later manipulation (Repovs and Baddeley, 2006; Baddeley, 2010). Traditionally, working memory has been linked to the prefrontal cortex, as neurons in this area show increased spiking when information

Received April 15, 2022; accepted July 12, 2022; First published September 28, 2022.
The authors declare no competing financial interests.

Author contributions: J.R.-L., A.E., M.W., and S.H. designed research; M.W. performed research; J.R.-L., A.E., and M.W. analyzed data; J.R.-L. and S.H. wrote the paper.

has to be transiently stored (Fuster and Alexander, 1971; D'Esposito and Postle, 2015). However, more recent research has shown that the brain mechanisms supporting working memory are not limited to the activity of individual neurons in a specific part of the cortex (Miller et al., 2018). Rather, memory traces are distributed in the brain, involving areas beyond the prefrontal cortex (Christophel et al., 2017, 2018). Moreover, the transient maintenance of information involves changes at network level that cannot be well addressed when studying the activity of single neurons (Miller et al., 2018). Neural oscillations, which reflect the summed activity of neural populations (Cohen, 2017), are thought to play an important role in the transient storage of information in the brain (Lundqvist et al., 2016, 2018; Wolinski et al., 2018).

In the human brain, neural oscillations are dominated by alpha rhythms (8–14 Hz; Hari et al., 1997; Bazanova and Vernon, 2014). Although alpha rhythms are most prominent in posterior areas, they are also found in sensorimotor and auditory cortex (commonly referred to as "mu" and "tau" rhythms, respectively; Lehtelä et al., 1997; Pfurtscheller et al., 2000; Haegens et al., 2011; Bastarrika-Iriarte and Caballero-Gaudes, 2019). Previous work has shown that alpha oscillations desynchronize (decrease in power) in task-relevant areas and synchronize (increase in power) in task-irrelevant areas in a wide variety of cognitive tasks (Klimesch, 1999; Jensen et al., 2002; Jokisch and Jensen, 2007; Haegens et al., 2009). Based on these results, it has been proposed that alpha's function is to gate information through the brain via functional inhibition (Klimesch et al., 2007; Jensen and Mazaheri, 2010). In line with this idea, recent research in humans demonstrates that the amplitude of alpha oscillations is negatively associated with neural excitability (Chapeton et al., 2019; Haegens et al., 2022; Iemi et al., 2022).

Posterior alpha oscillations are thought to be especially relevant in visual working memory (de Vries et al., 2020). Although several studies have shown significant power modulations of posterior alpha rhythms when visual information has to be transiently stored, the direction of these power modulations is highly inconsistent (Pavlov and Kotchoubey, 2022). Studies reporting increased alpha power during visual memory maintenance argue that this increase is aimed to block visual input by inhibiting (task-irrelevant) occipital and/or parietal areas (Jensen et al., 2002; Tuladhar et al., 2007; Bonnefond and Jensen, 2012). In contrast, studies reporting posterior alpha power decreases during memory retention argue that these occipitoparietal areas are actually task-relevant and need to be disinhibited to support the short-term storage of visual information (van Ede et al., 2017; de Vries et al., 2018; Erickson et al., 2019).

A possible explanation for the inconsistent findings regarding posterior alpha modulations during visual working memory is the existence of multiple alpha rhythms. More than 20 years ago, Klimesch and colleagues proposed a division of the alpha band in different sub-bands (i.e., "upper alpha" and "lower alpha") based on their differential power modulations during a wide range of cognitive tasks (Klimesch et al., 1993; Klimesch, 1999). However, since alpha rhythms were not spatially separated in these studies, it was not possible to assess whether power modulations in the two alpha sub-bands reflected the activity of two different oscillators or a change in frequency of a single oscillator (Haegens et al., 2014; Mierau et al., 2017). Later studies that did perform source separation supported the idea of multiple posterior alpha rhythms. Specifically, spatially distinct posterior alpha rhythms have been identified in the context of resting state (Barzegaran et al., 2017), visual perception (Gulbinaite et al., 2017; Benwell et al., 2019) and multimodal attention (Sokoliuk et al., 2019).

Previous literature has shown that independent component analysis (ICA) is a powerful analytical tool to separate brain rhythms in Magneto- and Electro-Encephalography (M/EEG) (Debener et al., 2005; Wagner et al., 2018; Benwell et al., 2019). ICA is a blind source separation technique that aims to identify signals whose time courses convey maximally distinct information. When applied to M/EEG data, ICA is thought to be able to separate locally synchronous activity from distinct "cortical patches" (i.e., compact neuronal populations with strong short-range anatomic connections; Onton et al., 2006). The main advantage of ICA relative to other source localization techniques is that it simplifies the M/EEG inverse problem by modeling which signals are contained in the volume conducted scalp data instead of estimating the projection weights of all possible sources (Delorme et al., 2012).

In this study, we use ICA to examine whether alpha power modulations in posterior regions during short-term memory retention reflect the activity of one or several brain rhythms. We acquired magnetoencephalography (MEG) during a visual working-memory task in which participants ($N = 33$) had to briefly remember one out of four spatial directions, while task difficulty was modulated by introducing visual distractors. We first assessed alpha dynamics at sensor level by comparing alpha power and frequency between fixation and memory retention. Then, we performed the same comparison using statistically independent posterior sources as extracted through ICA (Delorme et al., 2012). Interestingly, while results at sensor level suggested a change in power and frequency of a single posterior alpha rhythm during memory retention, our ICA results demonstrated that posterior alpha dynamics reflect the activity of at least two alpha rhythms with distinct functions and spatiospectral characteristics. We believe that these results have important implications not only for the analysis and interpretation of alpha oscillations in M/EEG but also for their potential modulation through different neurostimulation techniques.

This work was supported by The Netherlands Organisation for Scientific Research (NWO) Vidi Grant 016.Vidi.185.137 and by National Institutes of Health Grant R01-MH123679.

Correspondence should be addressed to Julio Rodriguez-Larios at juliorlarios@gmail.com.

https://doi.org/10.1523/ENEURO.0159-22.2022

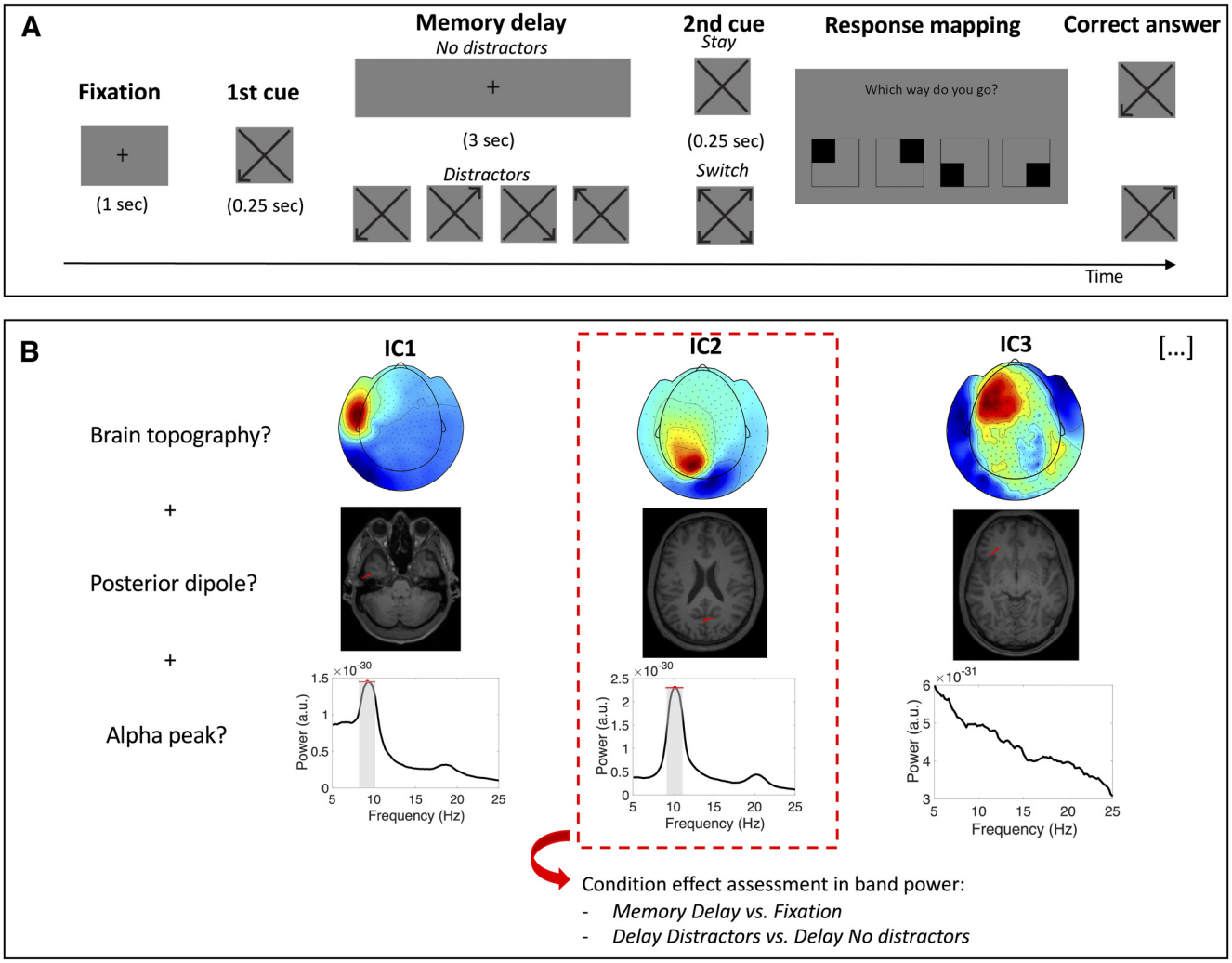

Figure 1. Task and main analytical approach. ***A***, Task schematic. Participants were asked to remember a visual direction cue (i.e., upper left, upper right, bottom left, or bottom right) for 3 s (memory delay). In 50% of the trials, the delay period contained four visual distractors. Based on the content of a second cue (i.e., "stay" or "switch"), participants had to report the direction of the first cue or its opposite. ***B***, ICA-based selection in an exemplary subject. A selection of independent components was performed based on their topography (top panel), estimated source (middle), and spectrum (bottom). Only independent components with a brain topography (IClabel algorithm classification $>$ 0.80), an estimated dipole in occipital or parietal cortex and a peak in the α range were selected for analysis (in this example, the component marked in the red rectangle). The frequency band of each independent component was defined based on the average spectrum (peak frequency and width; gray area). Condition-related modulations in band power (i.e., delay vs fixation, distractor vs no distractor) were assessed through single-trial analysis of each independent component.

Materials and Methods

Participants

A total of 35 healthy right-handed adult participants (mean age 25.2 years, range 20–33; 17 female, 18 male) took part in the experiment. Participants reported normal or corrected-to-normal vision and no history of neurologic or mental illnesses. Before the experiment, participants were informed about the MEG system as well as safety regulations and signed an informed consent form. The study falls under the general ethics approval (CMO 2014/288 "Imaging Human Cognition") in accordance with the Declaration of Helsinki. After participation, the participants received a monetary reward. Two participants were excluded because of technical problems during data acquisition.

Experimental design

MEG was recorded while participants performed a visual working memory task (Fig. 1*A*). This task was designed to emulate real-life situations in which participants would navigate in a city using directions that they had to keep in mind for a short period of time. The goal of the task was to remember one out of four directions. Participants were first presented with a visual direction cue (0.25 s) pointing to the upper left, upper right, bottom left, or bottom right. After a delay period (3 s), a second

cue was presented (0.25 s). The second cue was either a "stay" cue, meaning that the correct answer was the direction indicated by the first cue, or a "switch" cue, indicating that the correct answer was the direction opposite to the first cue. After the second cue, a response mapping diagram was shown, indicating which button corresponded to which direction. The correspondence between each button and direction was randomized between blocks (a total of eight different response mapping diagrams were shown). Participants were instructed to answer as quickly and as accurately as possible, with the right hand via a button press. In 50% of the trials, the delay period contained four distractors (randomly drawn direction cues) that were presented at a 0.33-s interstimulus interval. Participants were instructed to ignore the distractors and to keep only the first cue in mind. Participants performed eight blocks of 48 trials (~5 min each), with short breaks between blocks. Participants were seated upright in the MEG helmet and were instructed to keep their head position as stable as possible for the duration of the experiment. Before the MEG recording, participants performed a training block (16 trials) to make sure that they understood the task correctly. The experimental stimuli were programmed and presented with the software Presentation (version 18.0, Neurobehavioural Systems).

Data acquisition

MEG data were recorded with a 275-channel CTF MEG system with axial gradiometers at a sampling rate of 1200 Hz (CTF MEG systems, VSM MedTech Ltd.). Six channels were disabled because of permanent malfunction. In order to monitor the head position of the participants and to allow for adjustments to the original position in between blocks, the real-time representation of the participant's head position was monitored using three head localization coils at the right and left ear canals as well as the nasion (Stolk et al., 2013). These points were further used as offline anatomic landmarks to align the MEG data with structural images of the participant's brain for source reconstruction. Further, movement of the left eye was tracked during the experiment using an Eyelink eyetracker (SR Research Ltd.). After the experiment, the participant's head shape was digitized using a Polhemus 3D tracking device (Polhemus). In a separate session, an anatomic MRI scan of the participant's brain was recorded, unless the participant's scan could be obtained from the database of the institute. The MRI data were recorded with the 3T Siemens Magnetom Skyra MR scanner.

MEG analysis

MEG analysis was performed using the Fieldtrip toolbox (Oostenveld et al., 2011), EEGlab (Delorme and Makeig, 2004), and custom MATLAB scripts (version R2021a).

Preprocessing

The raw continuous data were downsampled to 300 Hz and epoched relative to the first cue (from −1.5 to +10 s). A band-stop filter was applied at 50, 100, and 150 Hz to remove line noise and its harmonics. The data were visually inspected to reject trials with artifacts (e.g., muscle artifacts, SQUID sensor jumps). Next, the data were bandpass filtered between 3 and 30 Hz (Butterworth IIR filter) and ICA was computed (i.e., EEGlab implementation of the infomax ICA algorithm by Bell and Sejnowski, 1995). Finally, the IClabel algorithm (Pion-Tonachini et al., 2019) was used to classify components in the categories Brain, Muscle, Eye, Heart, Line Noise, Channel Noise, and Other based on their spatial topography.

Sensor-level analysis

First, independent components that were classified as muscle, eyes, heart or channel noise by the IClabel algorithm with a probability higher than 80% were discarded. Further analysis was performed at sensor level after backprojecting the remaining components. We computed the planar representation of the MEG field distribution from the single-trial data using the nearest-neighbor method. This transformation facilitates the interpretation of the sensor level data as it makes the signal amplitude maximal above its source (as implemented in Fieldtrip functions *ft_meg_planar* and *ft_combine_planar*). The power spectrum of each channel between 5 and 25 Hz was obtained using a multitaper frequency transformation (*ft_freqanalysis*). This transformation was done separately for the fixation (1 s) and the memory delay period (1-s window centered in the delay period). The data were zero-padded to 5 s to obtain a frequency resolution of 0.2 Hz. alpha Band power was estimated as the mean power values between 8 and 14 Hz across trials. Individual alpha power and frequency were estimated using the MATLAB *findpeaks* algorithm (i.e., maximum peak between 8 and 14 Hz).

Component-level analysis

A series of conditions were imposed to select posterior oscillatory components in the alpha range. First, independent components had to be classified as brain components by the IClabel algorithm with a probability higher than 80%. Second, independent components had to show a maximum peak in the alpha range (as detected with the MATLAB *findpeaks* function). Third, independent components needed to project to a single dipole in occipital or parietal cortex. For that purpose, the whole brain was scanned with a single dipole to find the location where the dipole model was best able to explain the topography of each independent component (*ft_dipolefitting*). The source localization of dipoles was done using individual T1-weighted anatomic images of the participants' brains. For that, individual MRIs were first normalized in MNI space (*ft_volumenormalise*) and segmented (*ft_volumesegment*). Then a realistic single-shell headmodel was computed (*ft_prepare_headmodel)* based on the surface mesh obtained from the segmented MRI (*ft_prepare_mesh*; Nolte, 2003). Finally, to automatically identify dipoles that were located in occipital and parietal cortices we used the AAL atlas (Tzourio-Mazoyer et al., 2002) available in the Fieldtrip toolbox (Oostenveld et al., 2011). The frequency transformation of independent components was identical to the one used for sensor level analysis. The only difference is that

to estimate alpha power per condition in single trials, the individual alpha band was previously defined per component based on its average power spectrum (across trials; Fig. 1*B*). This approach was adopted to compensate for the lower signal-to-noise ratio of oscillatory activity when estimated in single trials. For visualization purposes, independent components were also transformed in the time-frequency domain (5–25 Hz) using Morlet wavelets of six cycles (function *BOSC_tf*; see Whitten et al., 2011).

A similar approach was adopted to estimate peak frequency in single trials. In this case, independent components were first filtered (MATLAB function *firl1*) around their individual alpha band, after which instantaneous frequency was estimated with the method developed in Cohen (2014). In short, instantaneous frequency was computed by multiplying the first temporal derivative of the phase angle time series (extracted through its Hilbert transform) by the sampling rate and dividing it by 2π. Then, a median filter was applied to the instantaneous frequency time series (10 steps between 10 and 400 ms) to attenuate non-physiological frequency jumps. Instantaneous frequency was averaged within the fixation period and the memory delay (1-s windows) to get an estimation of peak frequency in each period.

Statistical analysis

Behavioral data

Repeated-measures ANOVA was performed with the JASP software (Love et al., 2019), *post hoc* paired samples *t* test were performed in MATLAB R2021a. The effect size was estimated as eta squared (η^2) for the ANOVA and as Cohen's *d* for the *t* tests.

MEG data

The comparison of MEG parameters of interest between conditions was performed using paired samples and independent samples *t* tests (MATLAB R2021a implementation). For the comparison of the parameters of interest in independent components at single-trial level (i.e., power/frequency during memory retentions vs delay), we employed Wilcoxon signed-rank test (MATLAB R2021a) to minimize the effect of possible outliers because they are more likely to occur when analyzing single trials (Cohen and Cavanagh, 2011). In order to assess a possible relationship between MEG parameters and accuracy, a median split approach was adopted. In short, trials were divided into two groups based on the median of the MEG parameter (i.e., high and low alpha power) and mean accuracy was compared between "high" and "low" trials at group level (paired-samples *t* tests). We corrected for multiple comparisons using the false discovery rate (FDR) method (Benjamini and Hochberg, 1995). Effect size was estimated through Cohen's *d* estimate.

Data and code accessibility

MEG data and MATLAB scripts to reproduce our findings will be made publicly available through the Open Science Framework (OSF) webpage: https://osf.io/h56b3/.

Results

Behavioral performance

Mean accuracy was 87.5% across conditions (SD = 19.4). Repeated-measures ANOVA revealed a significant main effect of the factor distractor ($F_{(1,32)} = 11.54$; $p = 0.002$; $\eta^2 = 0.102$). *Post hoc* paired sample *t* tests showed that accuracy was greater for the no distractor than for the distractor condition ($t_{(32)} = -3.39$; $p = 0.0018$; $d = 0.59$). No main effect of rule (i.e., stay vs switch) or rule by distractor interaction was found.

Mean reaction time was 698 ms across conditions (SD = 255). Repeated-measures ANOVA revealed a main effect of rule ($F_{(1,32)} = 8.79$; $p = 0.006$; $\eta^2 = 0.12$). *Post hoc* paired sample *t* tests showed that reaction time was shorter for stay versus switch rules ($t_{(32)} = 2.96$; $p = 0.0057$; $d = 0.51$). No effect of distractor nor rule by distractor interaction was found. Note that since the decision-button association changed in each trial, reaction times are difficult to interpret in this task. For this reason, we focused on accuracy to assess brain-behavior associations.

Posterior alpha peak at sensor-level increases in power and decreases in frequency during memory retention

No significant differences between conditions in alpha power were found when estimated using an a priori definition of the alpha band (8–14 Hz; Fig. 2*A*, top plot). However, individual alpha peak power showed a significant increase during the memory delay in posterior and right frontocentral sensors ($p < 0.05$ after FDR correction; Fig. 2*A*, middle plot). In addition, individual alpha frequency decreased significantly in posterior and frontal sensors ($p < 0.05$ after FDR correction; Fig. 2*A*, bottom plot). Hence, some posterior sensors showed a significant modulation in both individual alpha peak power and frequency (Fig. 2*B*). No significant distractor effect (comparison of distractor vs no distractor conditions) or relation to accuracy (median split approach) were found in either individual alpha power or frequency at sensor level.

ICA reveals two distinct alpha components based on their power modulations during the memory delay

In order to assess whether the reported changes in posterior alpha power reflect the activity of one or several brain rhythms, we performed the same condition comparisons that we performed at sensor level using independent posterior alpha components (Fig. 1*B*). We found a total of 170 posterior alpha components (across subjects) based on their topography at sensor level, their spectrum, and their estimated source. The power of 111 components was significantly modulated during the memory delay relative to fixation ($p < 0.05$ after FDR correction; mean number of components per subject = 3.3; SD = 2.9). Unlike sensor-level analysis, the comparison of posterior alpha components in single subjects revealed both increases and decreases in alpha power during the memory delay. Specifically, the power of 68 alpha components showed a significant increase during memory delay relative to fixation (hereafter called Alpha1), while the power of 43

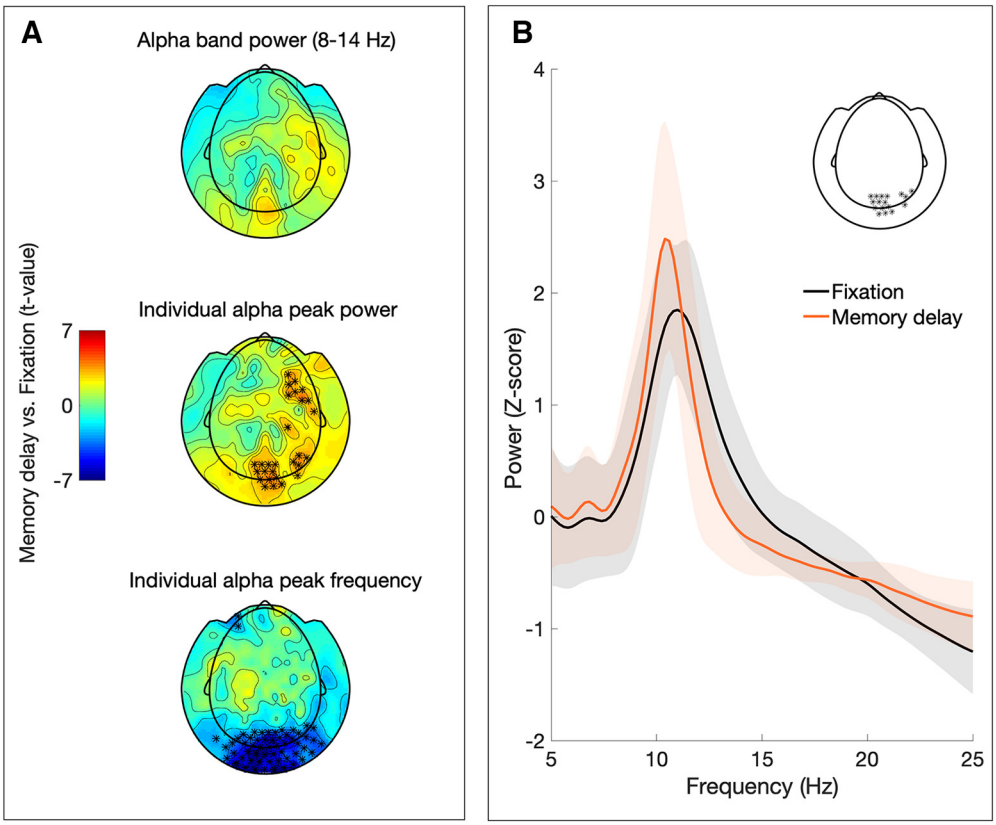

Figure 2. Sensor level analysis. ***A***, Topographic plots depicting the *t* values from the condition comparison (memory delay vs fixation) in α band power (top), individual α peak power (middle), and individual α peak frequency (bottom). Significant differences ($p < 0.05$ after FDR correction) are marked with asterisks. ***B***, Mean power spectrum for fixation (black graph) and memory delay (orange) of sensors showing significant changes in individual α peak power and frequency (shaded area depicts SD across subjects; sensors included in spectra indicated in inset).

alpha components showed a significant decrease (hereafter called Alpha2; Fig. 3*A*). The breakdown across subjects was as follows: nine subjects showed both types of alpha components, 11 subjects showed Alpha1 components only, seven subjects showed Alpha2 components only, and six subjects showed no significant alpha components.

In addition, we assessed whether the frequencies of Alpha1 and Alpha2 components were differentially modulated during memory delay. However, we did not find significant differences between Alpha1 and Alpha2 components in frequency modulations associated with memory retention ($t_{(109)} = -1.45$; $p = 0.14$; $d = 0.28$). Both Alpha1 and Alpha2 components significantly decreased in frequency during the memory delay relative to fixation ($t_{(67)} = -8.18$, $p < 0.001$; $d = 1.00$; $t_{(42)} = -6.98$, $p < 0.001$; $d = 1.07$).

In summary, single-subject analysis of posterior alpha components demonstrates the existence of at least two distinct rhythms (Alpha1 and Alpha2) based on their opposite power modulations during memory retention.

Alpha1 and Alpha2 show opposite distractor-related power modulations

In order to assess whether the power of Alpha1 and Alpha2 components was differentially modulated in the presence of distractors, we first estimated the distractor effect in individual components (distractor vs no distractor) through Wilcoxon signed rank tests. Then we tested at group level whether the z-values of Alpha1 and Alpha2 components differed significantly from 0 (one sample *t* test) and from each other (independent samples *t* test). We found that alpha components that increased in power during the memory delay (i.e., Alpha1) showed a significant power increase in the presence of distractors ($t_{(67)} = 2.66$; $p = 0.0097$; $d = 0.32$) while alpha components that decreased in power during the memory delay (i.e., Alpha2) showed a significant power decrease in the presence of distractors ($t_{(42)} = -5.78$; $p < 0.001$; $d = 0.88$). Hence, Alpha1 and Alpha2 showed opposite and significantly different ($t_{(109)} = 5.42$; $p < 0.001$; $d = 1.05$) distractor-related power modulations (Fig. 3*B*,*E*).

Alpha1 and Alpha2 power modulations have an opposite relation to accuracy

In order to assess the behavioral relevance of Alpha1 and Alpha2 power modulations, we compared the accuracy between trials with high and low alpha power during the delay (% change from fixation). Since the presence of distractors was associated with lower accuracy, we performed this analysis for distractor and no-distractor conditions separately. For the distractor condition, accuracy

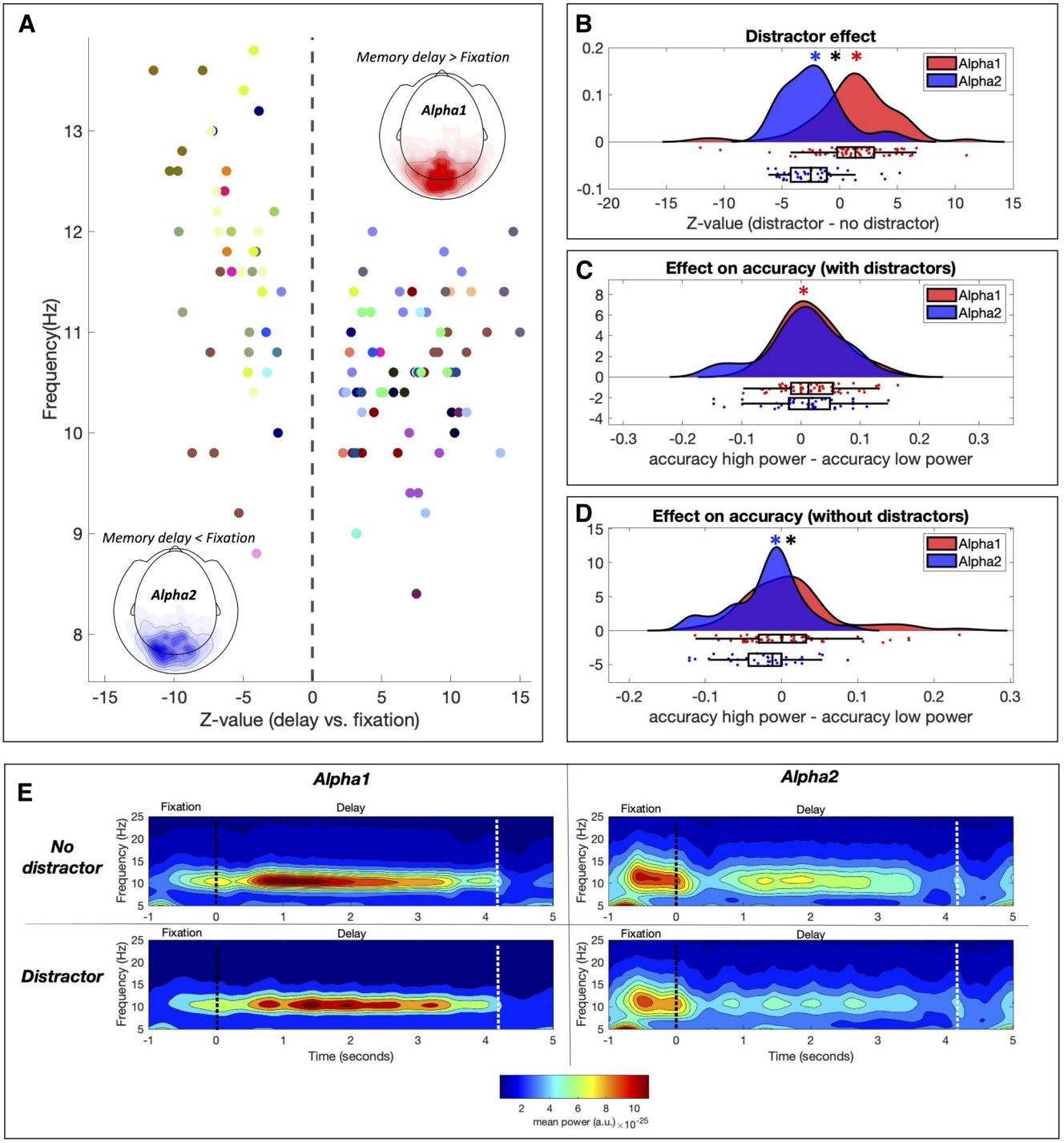

Figure 3. Power modulations of independent α components. ***A***, Power changes during the memory delay relative to fixation. Z-values (representing the memory retention effect in each component) are plotted as a function of their peak frequency (each color codes for a different subject). Components showing a significant increase in power during the memory delay were denominated Alpha1 while components showing a significant decrease were denominated Alpha2. The mean topography of the power change is plotted separately for Alpha1 (red) and Alpha2 (blue) components. ***B***, Differential distractor-related power modulations of Alpha1 and Alpha2 components. Z-values represent the distractor effect in individual components. At group level, Alpha1 components (red) showed significantly more power in the presence of distractors while Alpha2 components (blue) showed significantly less. Colored asterisks mark statistical significance ($p < 0.05$) of the Alpha1 (red) or Alpha2 (blue) distributions against 0 (one-sample *t* test). Black asterisks mark significant differences ($p < 0.05$) between Alpha1 and Alpha2 distributions. ***C***, Effect of power modulations on accuracy in the distractor condition. Accuracy was compared for high power and low power trials (median split), showing a significantly greater accuracy for trials with high Alpha1 power in the distractor condition. ***D***, Same as ***C*** for the no-distractor condition, showing a significantly lower accuracy for trials with high Alpha2 power in the

continued
no-distractor condition. ***E***, Average time-frequency representation of Alpha1 and Alpha2 components for the distractor and the no distractor conditions. The black vertical line indicates the presentation of the first cue. The white vertical line marks the presentation of second cue.

was significantly higher for trials showing greater Alpha1 power ($t_{(67)} = 2.97$; $p = 0.0041$; $d = 0.36$), while no differences were found in Alpha2 power ($t_{(42)} = 0.54$; $p = 0.58$; $d = 0.08$). However, power-related differences in accuracy between Alpha1 and Alpha2 did not reach statistical significance ($t_{(109)} = 1.18$; $p = 0.24$; $d = 0.23$). For the no-distractor condition, accuracy was significantly higher for trials with lower Alpha2 power ($t_{(42)} = -2.79$; $p = 0.0078$; $d = 0.42$), while no significant difference was found in Alpha1 power ($t_{(67)} = 1.42$; $p = 0.15$; $d = 0.17$). In this case, power-related differences in accuracy between Alpha1 and Alpha2 components did reach statistical significance ($t_{(109)} = 2.76$; $p = 0.0067$; $d = 0.53$).

In summary, in the presence of visual distractors, better accuracy was associated with higher Alpha1 power, while in the absence of visual distractors, better accuracy was associated with lower Alpha2 power.

Alpha1 and Alpha2 components differ in their spatiospectral characteristics

In order to assess whether Alpha1 and Alpha2 rhythms differ in their spatiospectral characteristics, we compared three different spectral parameters (peak frequency, peak width, and relative amplitude; Fig. 4*A*) and the location of their estimated main source through dipole fitting (*x*-, *y*-, and *z*-axes; Fig. 4*B*). This analysis revealed that Alpha1 components tended to have a lower peak frequency ($t_{(109)} = -6.00$; $p < 0.001$; $d = 1.16$), a narrower peak width ($t_{(109)} = -2.43$; $p = 0.016$; $d = 0.47$), a greater relative peak amplitude ($t_{(109)} = 5.68$; $p < 0.001$; $d = 1.10$), and a more central source estimation ($t_{(109)} = 2.86$; $p = 0.005$; $d = 0.55$) than Alpha2 components (Fig. 4*C*). No significant differences were found between the source estimation of Alpha1 and Alpha2 components in the other two axes (i.e., ventral to dorsal and posterior to anterior).

Discussion

In this study we used ICA to examine whether posterior alpha power modulations during visual working memory reflect the dynamics of one or several brain rhythms. We recorded MEG while participants ($N = 33$) performed a visual working-memory task in which one out of four spatial directions had to be remembered for a short period of time. Task difficulty was modulated by introducing visual distractors during memory retention. Group analysis at sensor level suggested that posterior alpha consists of a single oscillator that increases in power and decreases in frequency during memory retention. In contrast, the analysis of independent components in single subjects revealed the existence of an alpha rhythm that increases in power during the memory delay (Alpha1), and an alpha rhythm that decreases in power during the memory delay (Alpha2). Interestingly, the power of Alpha1 and Alpha2 rhythms was differentially modulated by the presence of distractors (Alpha1 increased in power while Alpha2 decreased) and had an opposite relationship with accuracy (positive for Alpha1 and negative for Alpha2). In addition, Alpha1 and Alpha2 rhythms differed significantly in their spatiospectral characteristics. Specifically, Alpha1 rhythms showed a lower peak frequency, a narrower peak width, a greater relative peak amplitude and a more central source than Alpha2 rhythms. Thus, our results show that modulations in posterior alpha oscillations during memory retention reflect the dynamics of at least two distinct brain rhythms with different functions and spatiospectral characteristics.

The existence of alpha rhythms that increase and decrease in power during memory retention depending on their spatial origin is in line with prevailing theories of alpha function (Klimesch et al., 2007; Jensen and Mazaheri, 2010). According to these theories, alpha power reflects local cortical inhibition and therefore should increase in task-irrelevant areas and decrease in task-relevant areas. In the context of memory retention, it can be predicted that brain regions that are relevant to the transient maintenance of visual information would show alpha power decrease (disinhibition). On the other hand, brain regions that are irrelevant for memory maintenance (and could potentially interfere with the task) would show alpha power increase (inhibition). Although source estimation through dipole fitting in M/EEG has to be interpreted with caution (Leahy et al., 1998), the spatial distribution of the two observed types of alpha components suggests that, at least in occipital cortex, Alpha1 rhythms mostly originate in early visual areas while Alpha2 rhythms localize to higher-order areas (Fig. 4*B*). This is supported by their spectral profiles, since higher-order areas are thought to show a more pronounced 1/f trend (Ibarra Chaoul and Siegel, 2021) and higher peak frequency (Lundqvist et al., 2020), i.e., in line with what we see in Alpha2 components when compared with Alpha1 (Fig. 4*A*). Based on these results and previous evidence (Tuladhar et al., 2007; Popov et al., 2017; de Vries et al., 2018), we speculate that Alpha1 power increases reflect the inhibition of lower-order areas involved in visual processing, while Alpha2 power decreases reflect the disinhibition of higher-order areas supporting the transient storage of visual information.

If Alpha1 and Alpha2 rhythms during memory retention reflect the inhibition and disinhibition of task-irrelevant and task-relevant areas respectively, we would expect that behavioral performance improves when Alpha1 power increases and Alpha2 power decreases. Interestingly, Alpha1 power increases and Alpha2 power decreases were associated with better accuracy in different experimental conditions. Specifically, Alpha1 power was positively associated with accuracy only in the presence of distractors, while Alpha2 power was negatively associated with accuracy only in the absence of distractors. We hypothesize that behavioral performance in distractor and no-distractor conditions depends on different factors. On the one hand, incorrect

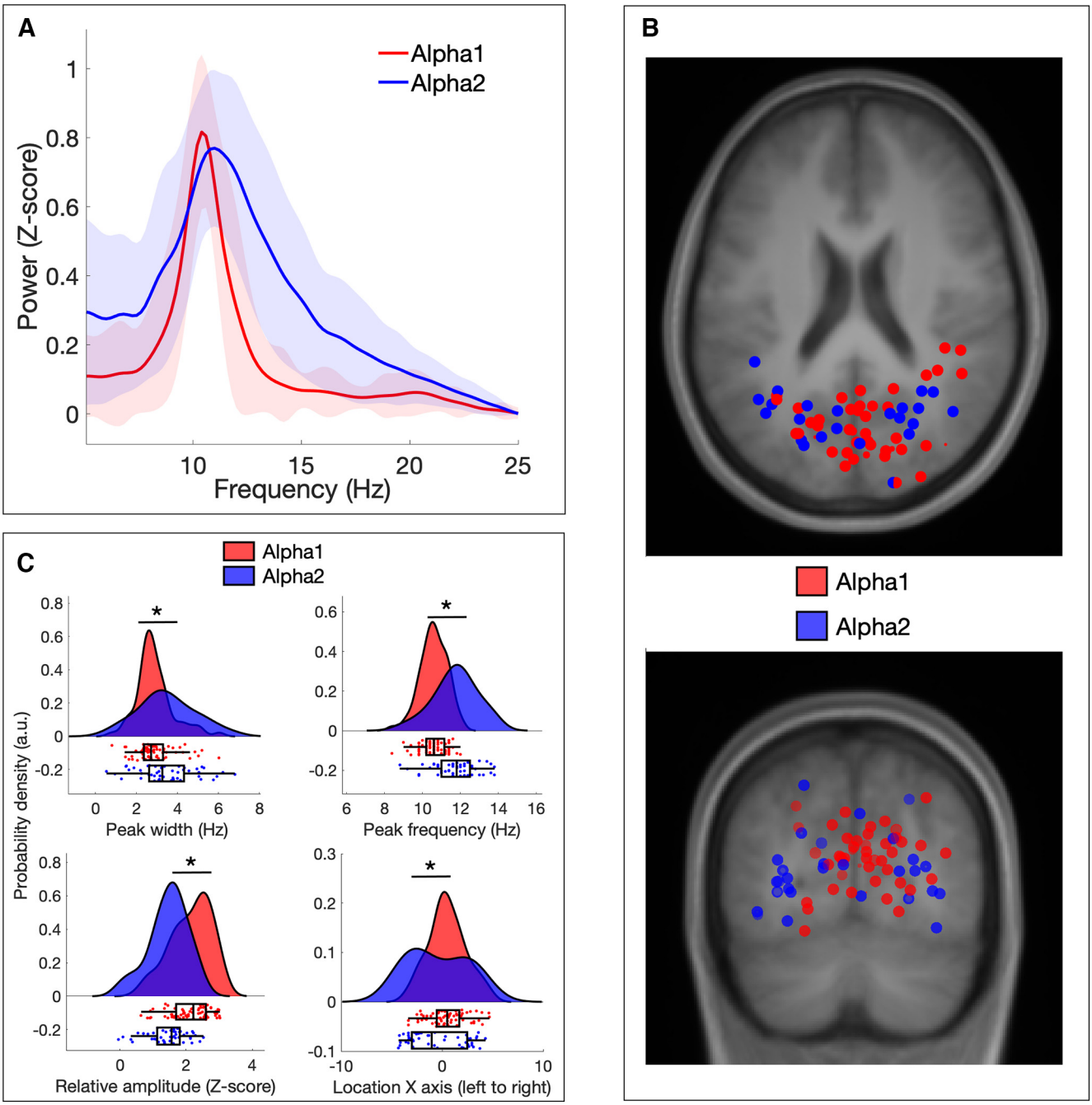

Figure 4. Spatiospectral differences between Alpha1 and Alpha2 components. ***A***, Average spectrum of Alpha1 and Alpha2 components across the complete trial (shaded area depicts SD). ***B***, Source localization of Alpha1 (red) and Alpha2 (blue) components as estimated through dipole fitting. The top panel shows the horizontal plane while the bottom panel shows the coronal plane. ***C***, Plots depicting significant differences in four spatiospectral parameters: peak width (top left panel), peak frequency (top right), relative amplitude (bottom left) and location (bottom right).

responses in the distractor condition might mostly be because of the interference of visual distractors. In this scenario, Alpha1 power increases become predictive of behavior because it inhibits areas involved in visual processing to avoid interference during memory retention. On the other hand, in the condition without distractors, incorrect responses might predominantly be caused by lapses of attention because of mind wandering and/or drowsiness (Braboszcz and Delorme, 2011; Andrillon et al., 2019, 2021; Rodriguez-Larios and Alaerts, 2021). Previous literature suggests that lapses of attention involve reduced cortical processing of external events (Smallwood et al., 2008). If an external event is not properly processed by the brain during an attentional lapse, its content cannot be maintained in working memory. Hence, we can expect that the recruitment of cortical areas supporting short-term memory retention (i.e.,

Alpha2 desynchronization) is less pronounced (or even absent) during an attentional lapse because there is little or no information to be retained. Nonetheless, it is important to note that the reported differences in accuracy depending on Alpha1/Alpha2 power modulations must be interpreted with caution because of the small number of incorrect trials (mean accuracy was 87% across conditions). In order to overcome this limitation in future work, it would be important to assess the here reported effects with a more difficult task or by adjusting task-difficulty at an interindividual level.

Recent literature points to the physiological and computational relevance of frequency modulations of neural oscillations (Cohen, 2014; Lowet et al., 2017; Klimesch, 2018). However, because of volume conduction, spurious frequency modulations at sensor level can emerge as a result of differential power modulation of multiple brain rhythms with distinct peak frequencies (Donoghue et al., 2022; Schaworonkow and Nikulin, 2022). Using ICA, we here demonstrate the existence of two distinct alpha rhythms in posterior cortex with different peak frequencies and opposite power modulations during memory retention. In light of these results, we cannot rule out the possibility that previously reported frequency changes in posterior alpha during different cognitive tasks (Angelakis et al., 2004; Haegens et al., 2014; Babu Henry Samuel et al., 2018; Rodriguez-Larios and Alaerts, 2019) are actually reflecting differential power modulations of multiple alpha rhythms with different peak frequencies. Therefore, future studies are needed to assess whether the previously reported alpha frequency changes in M/EEG during different cognitive tasks hold after the spatial separation of different alpha rhythms.

The spatial separation of different alpha rhythms could resolve some of the previous inconsistencies in the literature concerning the role of alpha phase, power and frequency in cognition (Samaha et al., 2020; Michail et al., 2022; Pavlov and Kotchoubey, 2022; Zazio et al., 2022). Similarly, separating different alpha rhythms could allow us to understand why some neurofeedback and neurostimulation protocols do not have the expected effect in some subjects (Orendáčová and Kvašňõák, 2021). If we tune the neurofeedback/stimulation parameters (and/or assess their effects) at sensor level, we cannot know whether we are modulating the power or frequency of one or several alpha rhythms. As different alpha rhythms could be more prominent in different subjects because of interindividual differences in brain anatomy and functional specialization, this might have a key impact on the effects of their modulation (Duffau, 2017; Mikkonen et al., 2020).

In conclusion, our results show that posterior alpha dynamics during memory retention reflect the activity of at least two brain rhythms with distinct functions and spatiospectral characteristics. Alpha1 rhythms increased in power during memory retention and in the presence of visual distractors, while Alpha2 rhythms showed the opposite power modulations. In addition, Alpha1 and Alpha2 rhythms had an opposite relationship with accuracy (positive for Alpha1 and negative for Alpha2). Lastly, Alpha1 and Alpha2 differed significantly in several spectral parameters (peak frequency, peak width and relative amplitude) and in the location of their estimated main source. In the light of previous results and theoretical accounts (Klimesch et al., 2007; Jensen and Mazaheri, 2010; Haegens et al., 2022; Iemi et al., 2022), we hypothesize that during memory retention, Alpha1 rhythms increase in power to inhibit visual processing while Alpha2 rhythms decrease in power to disinhibit areas supporting the short-term storage of visual information.

References

Andrillon T, Windt J, Silk T, Drummond SPA, Bellgrove MA, Tsuchiya N (2019) Does the mind wander when the brain takes a break? Local sleep in wakefulness, attentional lapses and mind-wandering. Front Neurosci 13:949.

Andrillon T, Burns A, Mackay T, Windt J, Tsuchiya N (2021) Predicting lapses of attention with sleep-like slow waves. Nat Commun 12:3657.

Angelakis E, Lubar JF, Stathopoulou S, Kounios J (2004) Peak alpha frequency: an electroencephalographic measure of cognitive preparedness. Clin Neurophysiol 115:887–897.

Babu Henry Samuel I, Wang C, Hu Z, Ding M (2018) The frequency of alpha oscillations: task-dependent modulation and its functional significance. Neuroimage 183:897–906.

Baddeley A (2010) Working memory. Curr Biol 20:R136–R140.

Barzegaran E, Vildavski VY, Knyazeva MG (2017) Fine structure of posterior alpha rhythm in human EEG: frequency components, their cortical sources, and temporal behavior. Sci Rep 7:8249.

Bastarrika-Iriarte A, Caballero-Gaudes C (2019) Closing eyes during auditory memory retrieval modulates alpha rhythm but does not alter tau rhythm. Neuroimage 197:60–68.

Bazanova OM, Vernon D (2014) Interpreting EEG alpha activity. Neurosci Biobehav Rev 44:94–110.

Bell AJ, Sejnowski TJ (1995) An information-maximization approach to blind separation and blind deconvolution. Neural Comput 7:1129–1159.

Benjamini Y, Hochberg Y (1995) Controlling the false discovery rate: a practical and powerful approach to multiple testing. J R Stat Soc Series B Stat Methodol 57:289–300.

Benwell CSY, London RE, Tagliabue CF, Veniero D, Gross J, Keitel C, Thut G (2019) Frequency and power of human alpha oscillations drift systematically with time-on-task. Neuroimage 192:101–114.

Bonnefond M, Jensen O (2012) Alpha oscillations serve to protect working memory maintenance against anticipated distracters. Curr Biol 22:1969–1974.

Braboszcz C, Delorme A (2011) Lost in thoughts: neural markers of low alertness during mind wandering. Neuroimage 54:3040–3047.

Chapeton JI, Haque R, Wittig JH, Inati SK, Zaghloul KA (2019) Large-scale communication in the human brain is rhythmically modulated through alpha coherence. Curr Biol 29:2801–2811.e5.

Christophel TB, Klink PC, Spitzer B, Roelfsema PR, Haynes JD (2017) The distributed nature of working memory. Trends Cogn Sci 21:111–124.

Christophel TB, Iamshchinina P, Yan C, Allefeld C, Haynes JD (2018) Cortical specialization for attended versus unattended working memory. Nat Neurosci 21:494–496.

Cohen MX (2014) Fluctuations in oscillation frequency control spike timing and coordinate neural networks. J Neurosci 34:8988–8998.

Cohen MX (2017) Where does EEG come from and what does it mean? Trends Neurosci 40:208–218.

Cohen MX, Cavanagh JF (2011) Single-trial regression elucidates the role of prefrontal theta oscillations in response conflict. Front Psychol 2:30.

D'Esposito M, Postle BR (2015) The cognitive neuroscience of working memory. Annu Rev Psychol 66:115–142.

de Vries IEJ, Van Driel J, Karacaoglu M, Olivers CNL (2018) Priority switches in visual working memory are supported by frontal delta and posterior alpha interactions. Cereb Cortex 28:4090–4104.
de Vries IEJ, Slagter HA, Olivers CNL (2020) Oscillatory control over representational states in working memory. Trends Cogn Sci 24:150–162.
Debener S, Ullsperger M, Siegel M, Fiehler K, von Cramon DY, Engel AK (2005) Trial-by-trial coupling of concurrent electroencephalogram and functional magnetic resonance imaging identifies the dynamics of performance monitoring. J Neurosci 25:11730–11737.
Delorme A, Makeig S (2004) EEGLAB: an open sorce toolbox for analysis of single-trail EEG dynamics including independent component analysis. J Neurosci Methods 134:9–21.
Delorme A, Palmer J, Onton J, Oostenveld R, Makeig S (2012) Independent EEG sources are dipolar. PLoS One 7:e30135.
Donoghue T, Schaworonkow N, Voytek B (2022) Methodological considerations for studying neural oscillations. Eur J Neurosci 55:3502–3527.
Duffau H (2017) A two-level model of interindividual anatomo-functional variability of the brain and its implications for neurosurgery. Cortex 86:303–313.
Erickson MA, Smith D, Albrecht MA, Silverstein S (2019) Alpha-band desynchronization reflects memory-specific processes during visual change detection. Psychophysiology 56:e13442.
Fuster JM, Alexander GE (1971) Neuron activity related to short-term memory. Science 173:652–654.
Gulbinaite R, İlhan B, Vanrullen R (2017) The triple-flash illusion reveals a driving role of alpha-band reverberations in visual perception. J Neurosci 37:7219–7230.
Haegens S, Osipova D, Oostenveld R, Jensen O (2009) Somatosensory working memory performance in humans depends on both engagement and disengagement of regions in a distributed network. Hum Brain Mapp 31:26–35.
Haegens S, Händel BF, Jensen O (2011) Top-down controlled alpha band activity in somatosensory areas determines behavioral performance in a discrimination task. J Neurosci 31:5197–5204.
Haegens S, Cousijn H, Wallis G, Harrison PJ, Nobre AC (2014) Inter- and intra-individual variability in alpha peak frequency. Neuroimage 92:46–55.
Haegens S, Pathak YJ, Smith EH, Mikell CB, Banks GP, Yates M, Bijanki KR, Schevon CA, McKhann GM, Schroeder CE, Sheth SA (2022) Alpha and broadband high-frequency activity track task dynamics and predict performance in controlled decision-making. Psychophysiology 59:e13901.
Hari R, Salmelin R, Mäkelä JP, Salenius S, Helle M (1997) Magnetoencephalographic cortical rhythms. Int J Psychophysiol 26:51–62.
Ibarra Chaoul A, Siegel M (2021) Cortical correlation structure of aperiodic neuronal population activity. Neuroimage 245:118672.
Iemi L, Gwilliams L, Samaha J, Auksztulewicz R, Cycowicz YM, King J-R, Nikulin VV, Thesen T, Doyle W, Devinsky O, Schroeder CE, Melloni L, Haegens S (2022) Ongoing neural oscillations influence behavior and sensory representations by suppressing neuronal excitability. Neuroimage 247:118746.
Jensen O, Mazaheri A (2010) Shaping functional architecture by oscillatory alpha activity: gating by inhibition. Front Hum Neurosci 4:186.
Jensen O, Gelfand J, Kounios J, Lisman JE (2002) Oscillations in the alpha band (9-12 Hz) increase with memory load during retention in a short-term memory task. Cereb Cortex 12:877–882.
Jokisch D, Jensen O (2007) Modulation of gamma and alpha activity during a working memory task engaging the dorsal or ventral stream. J Neurosci 27:3244–3251.
Klimesch W (1999) EEG alpha and theta oscillations reflect cognitive and memory performance: a review and analysis. Brain Res Brain Res Rev 29:169–195.
Klimesch W (2018) The frequency architecture of brain and brain body oscillations: an analysis. Eur J Neurosci 48:2431–2453.
Klimesch W, Schimke H, Pfurtscheller G (1993) Alpha frequency, cognitive load and memory performance. Brain Topogr 5:241–251.
Klimesch W, Sauseng P, Hanslmayr S (2007) EEG alpha oscillations: the inhibition-timing hypothesis. Brain Res 53:63–88.
Leahy RM, Mosher JC, Spencer ME, Huang MX, Lewine JD (1998) A study of dipole localization accuracy for MEG and EEG using a human skull phantom. Electroencephalogr Clin Neurophysiol 107:159–173.
Lehtelä L, Salmelin R, Hari R (1997) Evidence for reactive magnetic 10-Hz rhythm in the human auditory cortex. Neurosci Lett 222:111–114.
Love J, Selker R, Marsman M, Jamil T, Dropmann D, Verhagen J, Ly A, Gronau QF, Smíra M, Epskamp S, Matzke D, Wild A, Knight P, Rouder JN, Morey RD, Wagenmakers EJ (2019) JASP: graphical statistical software for common statistical designs. J Stat Soft 88:1–17.
Lowet E, Roberts MJ, Peter A, Gips B, De Weerd P (2017) A quantitative theory of gamma synchronization in macaque V1. Elife 6: e26642.
Lundqvist M, Rose J, Herman P, Brincat SL, Buschman TJ, Miller EK (2016) Gamma and beta bursts underlie working memory. Neuron 90:152–164.
Lundqvist M, Herman P, Warden MR, Brincat SL, Miller EK (2018) Gamma and beta bursts during working memory readout suggest roles in its volitional control. Nat Commun 9:394.
Lundqvist M, Bastos AM, Miller EK (2020) Preservation and changes in oscillatory dynamics across the cortical hierarchy. J Cogn Neurosci 32:2024–2035.
Michail G, Toran Jenner L, Keil J (2022) Prestimulus alpha power but not phase influences visual discrimination of long-duration visual stimuli. Eur J Neurosci 55:3141–3153.
Mierau A, Klimesch W, Lefebvre M (2017) State-dependent alpha peak frequency shifts: experimental evidence, potential mechanisms and functional implications. Neuroscience 360:146–154.
Mikkonen M, Laakso I, Tanaka S, Hirata A (2020) Cost of focality in TDCS: interindividual variability in electric fields. Brain Stimul 13:117–124.
Miller EK, Lundqvist M, Bastos AM (2018) Working memory 2.0. Neuron 100:463–475.
Nolte G (2003) The magnetic lead field theorem in the quasi-static approximation and its use for magnetoencephalography forward calculation in realistic volume conductors. Phys Med Biol 48:3637–3652.
Onton J, Westerfield M, Townsend J, Makeig S (2006) Imaging human EEG dynamics using independent component analysis. Neurosci Biobehav Rev 30:808–822.
Oostenveld R, Fries P, Maris E, Schoffelen JM (2011) FieldTrip: open source software for advanced analysis of MEG, EEG, and invasive electrophysiological data. Comput Intell Neurosci 2011:156869.
Orendáčová M, Kvašňõák E (2021) Effects of transcranial alternating current stimulation and neurofeedback on alpha (EEG) dynamics: a review. Front Hum Neurosci 15:628229.
Pavlov YG, Kotchoubey B (2022) Oscillatory brain activity and maintenance of verbal and visual working memory: a systematic review. Psychophysiology 59:e13735.
Pfurtscheller G, Neuper C, Krausz G (2000) Functional dissociation of lower and upper frequency mu rhythms in relation to voluntary limb movement. Clin Neurophysiol 111:1873–1879.
Pion-Tonachini L, Kreutz-Delgado K, Makeig S (2019) ICLabel: an automated electroencephalographic independent component classifier, dataset, and website. Neuroimage 198:181–197.
Popov T, Kastner S, Jensen O (2017) FEF-controlled alpha delay activity precedes stimulus-induced gamma-band activity in visual cortex. J Neurosci 37:4117–4127.
Repovs G, Baddeley A (2006) The multi-component model of working memory: explorations in experimental cognitive psychology. Neuroscience 139:5–21.
Rodriguez-Larios J, Alaerts K (2019) Tracking transient changes in the neural frequency architecture: harmonic relationships between theta and alpha peaks facilitate cognitive performance. J Neurosci 39:6291–6298.

Rodriguez-Larios J, Alaerts K (2021) EEG alpha-theta dynamics during mind wandering in the context of breath focus meditation: an experience sampling approach with novice meditation practitioners. Eur J Neurosci 53:1855–1868.

Samaha J, Iemi L, Haegens S, Busch NA (2020) Spontaneous brain oscillations and perceptual decision-making. Trends Cogn Sci 24:639–653.

Schaworonkow N, Nikulin VV (2022) Is sensor space analysis good enough? Spatial patterns as a tool for assessing spatial mixing of EEG/MEG rhythms. Neuroimage 253:119093.

Smallwood J, Beach E, Schooler JW, Handy TC (2008) Going AWOL in the brain: mind wandering reduces cortical analysis of external events. J Cogn Neurosci 20:458–469.

Sokoliuk R, Mayhew SD, Aquino KM, Wilson R, Brookes MJ, Francis ST, Hanslmayr S, Mullinger KJ (2019) Two spatially distinct posterior alpha sources fulfill different functional roles in attention. J Neurosci 39:7183–7194.

Stolk A, Todorovic A, Schoffelen JM, Oostenveld R (2013) Online and offline tools for head movement compensation in MEG. Neuroimage 68:39–48.

Tuladhar AM, ter Huurne N, Schoffelen J-M, Maris E, Oostenveld R, Jensen O (2007) Parieto-occipital sources account for the increase in alpha activity with working memory load. Hum Brain Mapp 28:785–792.

Tzourio-Mazoyer N, Landeau B, Papathanassiou D, Crivello F, Etard O, Delcroix N, Mazoyer B, Joliot M (2002) Automated anatomical labeling of activations in SPM using a macroscopic anatomical parcellation of the MNI MRI single-subject brain. Neuroimage 15:273–289.

van Ede F, Jensen O, Maris E (2017) Supramodal theta, gamma, and sustained fields predict modality-specific modulations of alpha and beta oscillations during visual and tactile working memory. J Cogn Neurosci 29:1455–1472.

Wagner J, Wessel JR, Ghahremani A, Aron AR (2018) Establishing a right frontal beta signature for stopping action in scalp EEG: implications for testing inhibitory control in other task contexts. J Cogn Neurosci 30:107–118.

Whitten TA, Hughes AM, Dickson CT, Caplan JB (2011) A better oscillation detection method robustly extracts EEG rhythms across brain state changes: the human alpha rhythm as a test case. Neuroimage 54:860–874.

Wolinski N, Cooper NR, Sauseng P, Romei V (2018) The speed of parietal theta frequency drives visuospatial working memory capacity. PLoS Biol 16:e2005348.

Zazio A, Ruhnau P, Weisz N, Wutz A (2022) Pre-stimulus alpha-band power and phase fluctuations originate from different neural sources and exert distinct impact on stimulus-evoked responses. Eur J Neurosci 55:3178–3190.